Desalination and Water Treatment
www.deswater.com
doi: 10.5004/dwt.2019.24337

162 (2019) 239–251
September

Kinetic, equilibrium isotherm and thermodynamic analysis for adsorption of Cr(VI) and Pb using powdered ground nut shell as a low-cost adsorbent

Deepak Sharma[a,b], Parmesh Kumar Chaudhari[a], Abhinesh Kumar Prajapati[b,*]

[a]*Department of Chemical Engineering, National Institute of Technology Raipur, Raipur 492001, India, emails: Deepak.ips86@gmail.com (D. Sharma), pkchaudhari.che@nitrr.ac.in (P.K. Chaudhari)*
[b]*Department of Chemical Engineering, Institute of Engineering and Science Indore, Indore 452001, India, Tel. +91-9713346092; email: abhineshgtk@gmail.com*

Received 16 November 2018; Accepted 25 April 2019

ABSTRACT

Agricultural waste peanut shell was used as precursor for activated carbon production by chemical activation. The activated carbon was prepared by carbonization of nut shell in a conventional electric furnace by a two-stage carbonization process under optimized conditions. The prepared carbons were characterized for proximate and ultimate analysis and thermodynamic characteristics. It was used for the removal of Cr(VI) and Pb contained in metal plating effluent by adsorption process. Experiments were performed in batch mode to find the effects of pH, contact time, particle size, adsorbent dose, initial concentration of adsorbate, and temperature. Cr(VI) and Pb adsorption was strongly depended on solution pH, and the optimum adsorption was found at pH 3.5. The maximum Cr(VI) removal of 94.4% (initial Cr(VI) = 55.3 mg/L) and Pb removal of 96.1% (initial Pb = 3.5 mg/L) were achieved at operating condition pH = 3, T = 25°C and adsorbent dose = 5 g/L. The kinetic data were evaluated at different initial concentrations of Cr(VI) and Pb using pseudo-first-order, pseudo-second-order, and intraparticle diffusion models. Among these, the pseudo-second-order model fitted well. Langmuir, Freundlich, and Temkin isotherms were also tested for equilibrium studies, in which Langmuir adsorption isotherm model fitted the data better. The thermodynamic parameters, such as standard enthalpy change ($\Delta H°$), Gibb's free energy change ($\Delta G°$), and standard entropy change ($\Delta S°$) were also evaluated.

Keywords: Peanut shell; $ZnCl_2$; Isotherm; Cr(VI); Pb; Kinetic models

1. Introduction

In the last few decades, the world has been facing challenge of potable water availability. Most of the drinkable water is supplied either from the rivers or from ground water. These water sources are polluted in terms of metal ion contamination, especially with chromium, cadmium, copper, lead, nickel, and zinc which causes serious problem if it enters living bodies. Cr(VI) and Pb are toxic at high concentrations. Pollution from these metals are seen frequently in municipalities and specific industries throughout the world. Among various sources of metal pollutants, the electroplating industries are on top.

Electroplating is a process where thin protective layer of a metal such as Zn, Cr, Ni, etc. is placed on the surface of a metal object using electrochemical process. During the process, some amount of coating materials do not deposit on the given object, which comes out with process stream in the form of effluent. This wastewater is commonly known as metal plating effluent (MPE). MPE contains several heavy metals such as Cr, Zn, Pb, etc. If MPE is directly discharged into any waterbody it can damage aquatic system.

* Corresponding author.

In addition, these heavy metals may be involved with food chain, consequently may lead to several diseases occurring in human body. Therefore, its proper treatment is required before discharge in any water source or surface of earth. World health organization has fixed the standard limit for chromium (0.1 mg/dm^3) and lead (0.1 mg/dm^3) to discharge in pure water stream [1].

A successful removal of heavy metals from water or wastewater is so difficult. Several physical or chemical processes can be used for this, however, the commercial uses of these processes are so difficult in terms of cost and removal efficiency effect. For example, traditional coagulation and electrocoagulation method is low cost but its removal efficiency is low and also generates a large amount of sludge. The membrane separation process is effective, but process cost is high. The adsorption process is one of the efficient method to remove heavy metals from MPE [2,3]. This process has several advantages as compared with other methods due to the excellent removal efficiency of some adsorbent such as activated carbon.

Number of materials such as coal, lignite, coconut shells, wood and peat has been used in the production of commercial activated carbons [4–6]. Recently some new biosorbent materials such as *Swietenia mahagoni* fruit shell (SMFS) [7], dried fungal biomass (*Trichoderma harzianum*) [8], *Strychnos nux-vomica* fruit shell has been also reported to treat different type of wastewater [9]. India is the second largest producer of groundnuts in the world, thus, there is great potential to use its shell. Groundnut shell is a carbonaceous, fibrous solid waste, which creates a disposal problem and is generally used as fuel. Therefore, it has developed the interest to prepare a valuable product, such as activated carbon. Groundnut shell having several advantages as greater percentage of non-carbon constituents in their composition compared with coal or peat, and it has better opportunity of retaining functional groups, especially oxygenated groups in the carbonized product [10]. Consequently, groundnut shell prepared activated carbon has more chances to provide better results as compared with traditional coal or peat prepared activated carbon. A comparison of adsorption capacity for Cr and Pb using different adsorbents are presented in Table 1. The aim of this work is to study the feasibility of developing an efficient adsorbent from groundnut shell along with $ZnCl_2$ activation, and to investigate its adsorption capacity for removal of Cr(VI) and Pb from MPE. Different parameters such as contact time, adsorbent doses, pH, temperature, etc. were tested to find the efficiency of prepared adsorbent. As per open literature available, the combined removal of Cr and Pb using peanut shell activated carbon adsorbent has been presented for the first time.

2. Materials and methods

2.1. Raw material

MPE was collected from the local metal plating industry, Indore (India) and stored in a deep freezer. Cr(VI) and Pb concentration were determined by atomic absorption spectrophotometer (AAS) (model AA-6200, Shimadzu made, Japan). Groundnut shell was obtained from the Indore local market. It was used as a precursor for the preparation of powdered activated carbon. Nut shell was properly washed to remove any mud followed by drying and then ground to a desired particle size for the further process of carbonization.

2.2. Preparation of adsorbent

The washed groundnut shell was carbonized in an electric furnace using two-stage carbonization process under optimized condition. Biomass waste was placed in a covered stainless steel vessels and carbonized at 400°C for 30 min in a muffle furnace (Labtech, Made, India) followed by chemical activation by impregnating $ZnCl_2$ for 24 h at a $ZnCl_2$/char ratio 1.75 and dried at 105°C. Later on, the dried and Zn impregnated char was carbonized at 650°C for 15 min. Before the utilization of prepared material (activated product), it was treated with 1:1 HCl for the removal of impregnating salt followed by washing with hot distilled water for the removal of chlorides and acidity [9].

2.3. Adsorbent characterization

The prepared activated carbons were analyzed for their moisture content, ash content, volatile matter, and fixed carbon (by difference) using the standard method as described in IS: 1350 (Part 1), 1984 [21]. Ultimate analysis was done by using CHNS analyzer (PerkinElmer Made, England).

2.4. Adsorption and kinetic studies

All the adsorption experiments were performed using batch technique. The liquid-phase adsorption capacity of the prepared carbon were examined by contacting 50 mL of MPE with 0.1 g activated carbon in 250 mL conical glass flask placed in a thermostated shaker (Model Max Q 4000, India) at 150 rpm. The pH of MPE was adjusted using dilute solution of HCl or NaOH. During the experiments, the effects of different parameters such as contact time, adsorbent dose, particle size, metal concentration, temperature, and initial pH of MPE on the adsorption process were studied. To achieve accuracy of the data, experiments were repeated whenever required. The Cr(VI) and Pb were determined by using AAS.

The amount of Cr(VI) and Pb removed per unit weight of adsorbent, q_e (mg/g) was calculated by the following equation:

$$q_e = \frac{V\left(C_0 - C_e\right)}{W \times 1{,}000} \tag{1}$$

where V is the volume of MPE in liter, C_0 and C_e are the initial and final concentrations (mg/L) of Cr(VI) and Pb in MPE, W is the weight (g) of adsorbent.

2.5. Equilibrium and kinetic studies

The different equilibrium adsorption isotherms were determined using batch studies. Equilibrium studies were performed at Cr(VI) initial concentration range 25–85 mg/L and Pb initial concentration range 3.5–17.5 mg/L in a series of 250 mL conical, Borosil glass flasks. Each flask was filled with 50 mL effluent and adjusted to the desired pH and

Table 1
Comparison table for the monolayer adsorption capacity for Cr and Pb using different adsorbents

S. No	Investigator	Adsorbent used	Metal removed	Initial concentration (mg/L)	% Metal removal
1	Naushad et al. [11]	YVO4:Eu^{3+} nanoparticles	Cd	25–200 mg/L	82
2	Mittal et al. [12]	Multiwalled carbon nanotubes (MWCNTs) were chemically modified to form nanocomposite with thorium oxide.	Pb	5 to 75 mg/L	94.6
3	Naushad et al. [13]	Ti(IV) iodovanadate cation exchanger	Pb and Hg	10–60 mg/L	Pb = 95 Hg = 65
4	Naushad et al. [14]	EDTA-Zr(IV) iodate composite cation exchanger	Pb	2–6	96
5	Naushad et al. [15]	Curcumin formaldehyde resin (CFR)	Cd	100 mg/L	91.1
6	Gutha et al. [16]	(Tomato) leaf powder	Ni	30–90 mg/L	58.82 mg/g
7	Bushra et al. [17]	Polyaniline Sn(IV) tungstomolybdate nanocomposite (PSTM)	Pb	10–30 mg/L	88
8	Naushad [18]	Nano-composite cation exchanger sodium dodecyl sulfate acrylamide Zr(IV) selenite (SDS-AZS)	Pb	10–30 μg/mL	90 [18]
9	Ghasemi et al. [19]	Fig sawdust activated carbon (FSAC)	Pb	100 mg/L	95.8
10	Ghasemi et al. [20]	Ash and Fe nanoparticles loaded ash (nFe-A)	Pb	50 mg/L	76.4 (Ash) 84.9 (nFe-A)
12	Present study	Ground nut activated carbon	Pb Cr	3.5 mg/L 55.3 mg/L	96.1 94.4

temperature. Prepared adsorbent was added to each flask and kept in isothermal shaker at 150 rpm until equilibrium was reached. In between the samples were withdrawn to find Cr(VI) and Pb in MPE at certain intervals. After 150 min, Cr(VI) and Pb concentration was not reduced much. The contact time of 250 min was used to achieve the equilibrium. The effect of temperature on adsorption was studied 20°C, 25°C, 30°C, 35°C, and 40°C. The same technique was employed for kinetic tests as that used for equilibrium experiments. The kinetic studies for Cr(VI) and Pb adsorption were carried out for four different initial Cr(VI) and Pb concentrations as discussed above at pH 3.5 and 25°C (room temperature).

3. Results and discussion

3.1. Characterization of adsorbents

The characteristics of activated carbon prepared from peanut shells by carbonization at 400°C and chemical activation with $ZnCl_2$ are listed in Tables 2–4. It is apparent from Table 2 that the activated carbon is acidic (pH 5.4) in nature along with high carbon content (83.31 wt.%). The specific surface area (S_{BET}) and micropore volume (V_{D-R}) of the prepared adsorbent sample was evaluated to 812.43 m^2/g and 0.85 cc/g, respectively. This value is much better than uncarbonized carbon [22]. Which may be due to after carbonization of peanut shell, its structure is disturbed and surface area is expanded, and pore volume and pore area also increased as data are presented in Table 4. It can be seen from the table that the specific surface area (S_{BET}), micropore surface area (S_{D-R}), and micropore volume (V_{micro}) of prepared carbon is good. This is due to carbonization facilitated the evolution of volatile matters from the raw peanut shell, and thereby enhanced the porosity in the carbon texture which resulted the increase in specific surface area and micropore surface area.

Table 2
Ultimate and proximate analysis of powdered ground nut shell adsorbent

Proximate analysis (weight %)		Ultimate analysis (dry basis) (weight %)	
Moisture	7.31	Carbon	73.4
Volatile matter	12.89	Hydrogen	4.23
Ash	10.2	Nitrogen	0.86
Fixed carbon	69.6	Sulfur	0.39

X-ray diffraction (XRD) technique is a powerful technique to analyze the crystalline and amorphous nature of the material. In crystalline material, well-defined peaks are observed, whereas in non crystalline or amorphous material no peaks are observed. The prepared carbon was also characterized by using an XRD machine with 2θ values ranging from 0° to 100°. The phase along with purity of the products was also examined by XRD. The XRD patterns of prepared carbon are shown in Fig. 1. The successive peaks can be observed at 20° and 50°, which indicates high purity of the prepared carbon. The most intense peak is at 28° and 40°. It is clear that the product is crystalline in nature.

SEM study was also carried out of the prepared carbon. This study is mostly done to see the morphological structure of the material. Fig. 2a presents the SEM image of prepared carbon. It is clear from the image that outer surface of the material is rough and different sizes of porous structure is available. Fig. 2b presents the SEM image of adsorbent

after the treatment of effluent, which indicates that the inside cavities of the porous structure is filled with Cr(VI) and Pb ions. The pore walls of the prepared carbon have narrow pores which creates higher surface area and adsorption capacity.

Thermal degradation (oxidation) characteristics of activated carbon obtained after adsorption process was studied by means of thermogravimetric (TG), differential thermogravimetric (DTG), and differential thermal analysis (DTA) tests in oxidative (air) environment. The result is presented in Fig. 3. This curve indicates a weight loss of 21.85% of its original weight up to 400°C. Between 400°C and 700°C, the sludge was further oxidized and has a weight loss of 6.5% of its original weight. Between 700°C and 800°C, only 4.18% weight loss was observed. The DTG curve displays a maximum rate of weight loss of 288 μg/min at 444°C. Another peak at 575°C indicates a weight loss of 242 μg/min. Thermal degradation is an exothermic reaction with a heat evolution of 1,330 kJ/kg at a temperature of 450°C (DTA curve). The results of TGA shows that the adsorbent can be burned and latter on the ash obtained can be used for land filling. The moderate heat was evaluated during the burning process.

Table 3
Physico-chemical characteristics of powdered ground nut shell prepared from $ZnCl_2$ activation of peanut shell

Parameters	Powdered ground nut shell adsorbent
pH	5.4
C (weight %)	83.31
H (weight %)	1.46
N (weight %)	0.33
O (weight %)	14.9
Yield %	34.12
Bulk density (g/cm^3)	0.38

Table 4
Surface area and pore volume analysis of oxidized and unoxidized activated carbon samples

Sample	Powdered ground nut shell adsorbent
Surface area (S_{BET}), m^2/g	812.43
Average pore width (DR), (Å)	110.56
Micropore volume (DR), (cc/g)	0.85
Micropore surface area (DR), (m^2/g)	1,221.55
Pore diameter (BJH), (Å)	35.63
Surface area (BJH), (m^2/g)	566.12
Pore volume (BJH), (cc/g)	0.88
Mesopore volume (cc/g)	0.061

3.2. Adsorption studies

3.2.1. Effect of initial pH

Activated carbons have dual nature, their surface is either positively charged or negatively charged, depending upon the solution pH [23]. It also contains a number of functional groups such as alkene, aldehyde, etc. The adsorption of heavy metals are related to the type and ionic state of these functional groups. In addition, the ionic state of metals, solubility of metals and degree of its ionization varied with pH, hence the pH of an effluent is one of the mandatory parameter for the removal of heavy metals [24]. Therefore, effect of pH on the removal of Cr(VI) and Pb was investigated over different pH range of 2–9.5 and room temperature 25°C and the initial concentration of Cr = 55.3 mg/L and Pb = 3.5 mg/L. Fig. 4a gives the effect of pH on removal of Cr(VI) and Pb. It can be seen from the figure that the adsorbent has provided better removal efficiency in the acidic range, and maximum adsorption occurred at pH 3.5 for both Cr(VI) and Pb. Thereafter, the removal efficiency was decreased with increase in pH, and at basic pH negligible

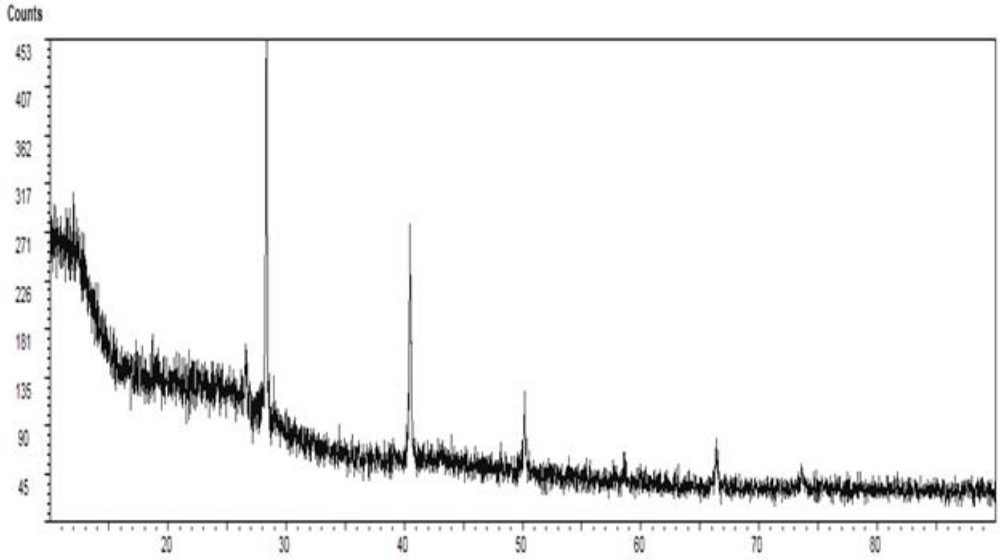

Fig. 1. X-ray diffractogram of prepared carbon.

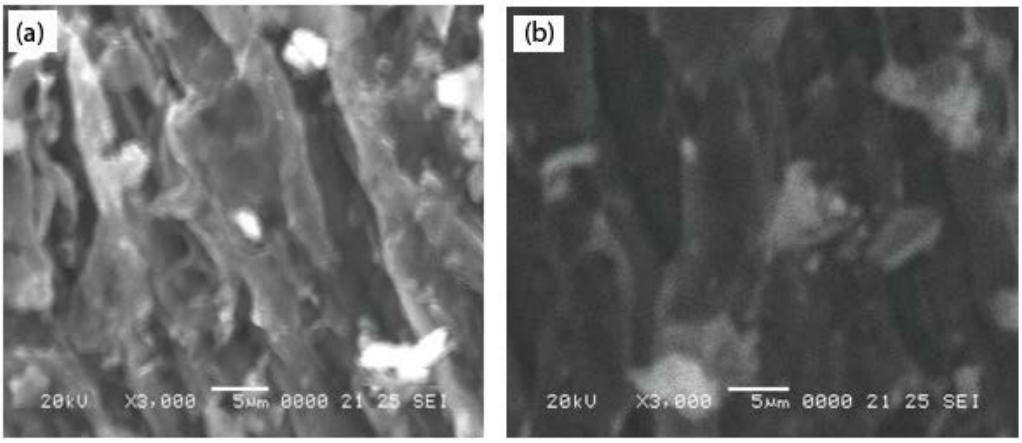

Fig. 2. Scanning electron microscope (SEM) images of (a) prepared adsorbent and (b) post treated adsorbent.

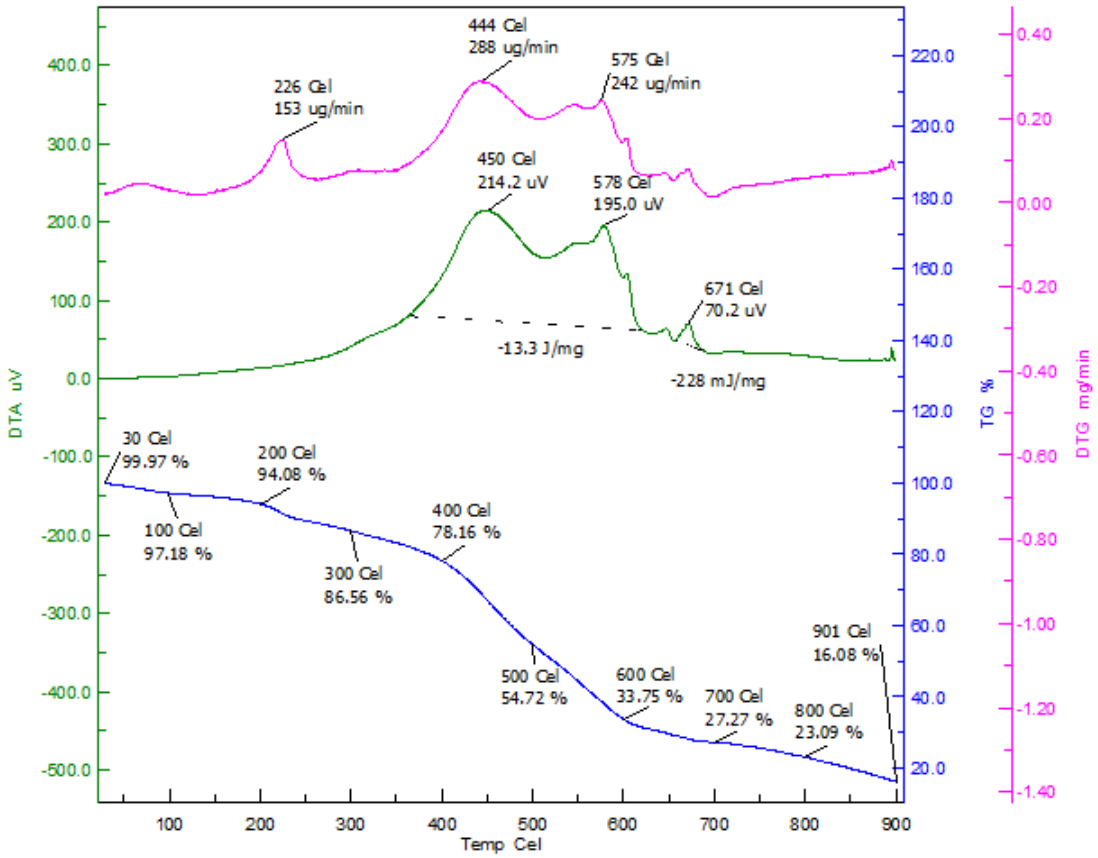

Fig. 3. TG, TGA, and DTA of used adsorbent.

metal removal was observed. At pH 3.5, the removal of Cr(VI) was 78.3% and Pb was 87%, which reduced to 25.41% and 21.78% at pH 9.5. In MPE, the Cr (VI) and Pb may exist in different ionic forms ($HCrO_4^-$, $Cr_2O_7^{2-}$, CrO_4^{2-}, PbO), which are present in unstable form, and stability of these ions is mainly based on the effluent pH [25]. It is well known fact that at the highly acidic pH, there is large number of H^+ ions occurred, which neutralized the negatively charged adsorbent surface [26], consequently increase in diffusion of chromate and Pb into bulk of adsorbent and increase in the removal of Cr(VI) and Pb. Apart from this, the decrease in adsorption at higher pH may be due to the increase in OH^- ions in the bulk, which retarded the diffusion of chromate ions and Pb ions [27]. As pH increases, the overall surface charge of the cell becomes negative and hence binding capacity decreases [28]. At near to neutral pH, the Pb contain in four oxidation stage, which changes to two oxidation stage at acidic pH. The formation of lead oxides is

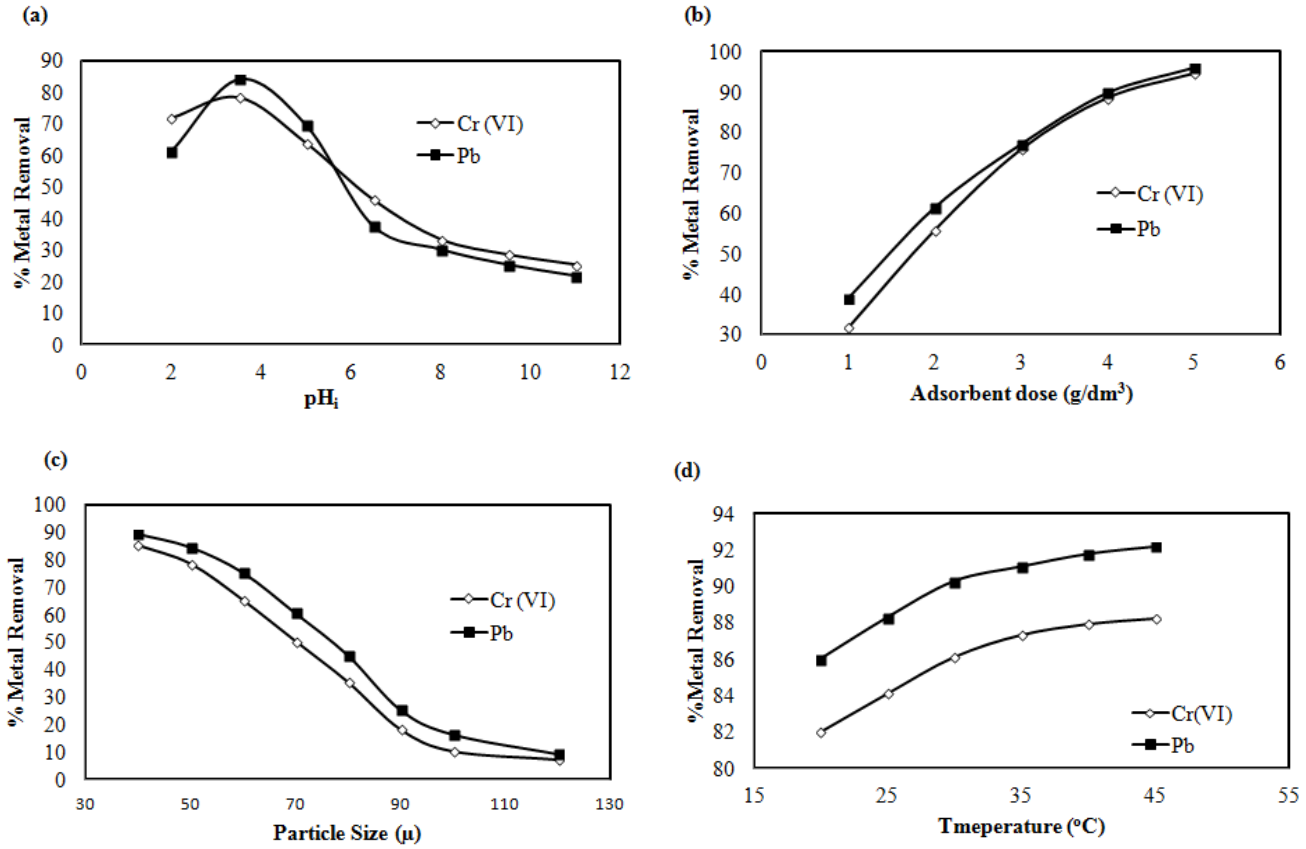

Fig. 4. Cr(VI) and Pb removal by adsorption (a) Effect of pH at 25°C, (b) effect of adsorbent dose at pH 3.5 and 25°C, (c) effect of particle size at pH 3.5 and 25°C, and (d) effect of temperature at pH 3.5.

expected by reaction of lead with dissolved oxygen at high acidic pH. The lead sulfate ($PbSO_4$) could be also form at low pH in presence of sulfate anions, which is quite insoluble [29]. Due to all these, removal of Cr(VI) and Pb was affected. Similar types of results were found by ALOthman et al. [27] and Maheshwari and Gupta [30]. Hence, pH 3.5 was selected as the optimal pH for further work on Cr(VI) and Pb adsorption on prepared adsorbent.

3.2.2. Effect of adsorbent dosage

The adsorbent dose also plays an important role on removal of heavy metals from the MPE [31,32]; therefore, experiments were conducted at different adsorbent dose, the results of metal removal are presented in Fig. 4b. It can be seen from the figure that Cr(VI) removal was increased from 31.6% to 94.5% and Pb removal was also increased from 39.1% to 96.1% with increase in adsorbent dose from 1 to 5 g/L. This is due to fact that, the higher adsorbent dose provides more surface area for adsorption. Percentage removal rate of both Cr(VI) and Pb became slow after a certain adsorbent mass load.

3.2.3. Effect of particle size

The adsorption of Cr(VI) and Pb at different size of adsorbent (40–120 μM) was also studied keeping initial concentration of Cr(VI) 55.3 and Pb 3.5 mg/L along with adsorbent dose 3 g/L. The results are presented in Fig. 4c. The adsorption capacity was found to decrease with increase in particle size of adsorbent. The removal of Cr(VI) was found to increase from 7.1% to 85.2% and Pb 9.2% to 89.1% with decrease in adsorbent size from 120 to 40 μM. It is well known fact that adsorption is a surface phenomenon and adsorption capacity is proportional to the surface area. The low particle size has much surface area; due to this high removal was found at low particle size. Similar kinds of results were observed by other researchers [33,34].

3.2.4. Effect of temperature

Temperature is a surrogate parameter in adsorption process. Hence the effect of temperature on adsorption process was studied at six different temperatures and results are presented in Fig. 4d. At 20°C Cr(VI) and Pb removal were achieved to be 84.18% and 88.3% which continued to increase up to 88.2% and 92.2% at 45°C. This may be due to the fact that temperature incorporates two major effects during adsorption process. Increase in the temperature increases the rate of diffusion of the adsorbate molecule across the external boundary layer and in the internal pores of the adsorbent particles. Variation in the temperature causes change in the equilibrium capacity of particular adsorbate [35]. Present adsorption process

may be endothermic in nature, therefore, with increase in temperature, adsorption capacity of adsorbent increased.

3.2.5. Effect of contact time and initial concentration

The adsorption of Cr and Pb with respect to contact time at various initial concentration is presented in Figs. 5a and b, respectively. The experiments were performed using prepared carbon at different initial concentration of Cr(VI) (25–85 mg/L) and Pb (3.5–17.5 mg/L) at desired pH (3.5) and temperature (25°C). It can be seen from Fig. 5, that the amount of Cr(VI) and Pb adsorbed were increased with increase in contact time. In addition, the uptake of heavy metal was fast in the first 60 min, thereafter rate of adsorption decreased and finally equilibrium point was observed. The saturation point was found near to 160 min for Cr(VI) and 150 min for Pb adsorption. Up to 60 min, the fast adsorption of Cr(VI) and Pb ions are due to availability of the uncovered surface and active sites on the adsorbent [22]. The amount of Cr(VI) and Pb ions adsorbed during the equilibrium show the maximum adsorption capacity of the adsorbent. The removal efficiency of Cr(VI) and Pb depended on the initial concentration of heavy metals. It can be seen that for different initial concentration of metals, at equilibrium, the amount of Cr(VI) adsorbed increased from 8.75 to 19.8 mg/g. The amount of Pb adsorbed increased from 1.23 to 4.1 mg/g. It is due to availability of active surface for adsorption. Similar type of result has been reported by Rangabhashiyam et al. [36].

3.3. Adsorption kinetics

Kinetics of adsorption process gives useful information about the reaction pathways and mechanism of the reactions; therefore, studies have been made for adsorption kinetics. For this, the pseudo-first-order, pseudo-second-order, and intraparticle diffusion models were studied. All models were successfully applied for the conformation between experimental data and the model predicted values as correlation coefficients (R^2). In present studies, higher value of R^2 indicates that the models are able to describe the kinetics of Cr(VI) and Pb adsorption.

3.3.1. Pseudo-first-order equation

The pseudo-first-order equation for solid–liquid systems could be represented as [37] follows:

$$\log\left(q_e - q_t\right) = \log q_e - \frac{k_1 t}{2.303} \tag{2}$$

where q_t and q_e are the amounts of Cr(VI) and Pb adsorbed (mg/g adsorbent) at time t and at equilibrium, k_1 is the rate

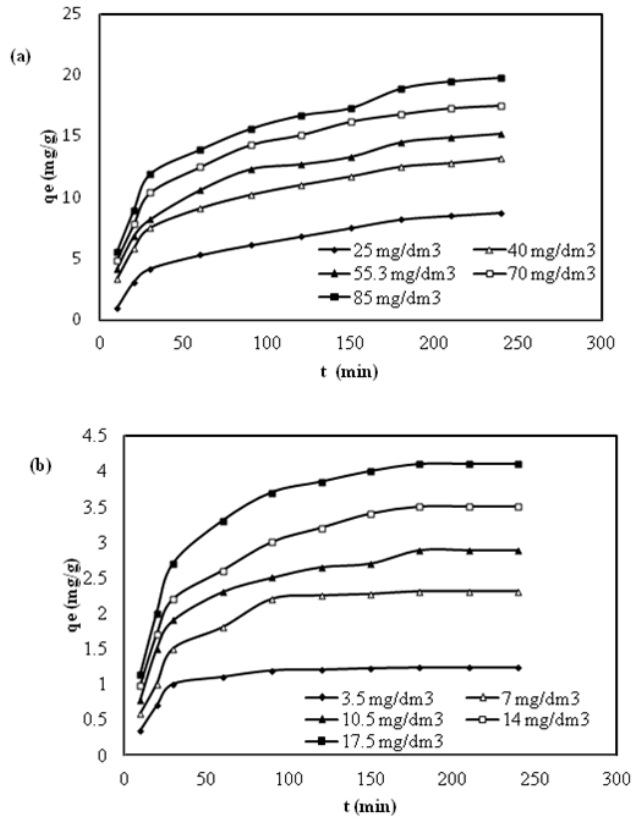

Fig. 5. Effect of contact time on (a) Cr(VI) removal and (b) Pb removal at different initial feed concentration. pH = 3.5, temperature = 25°C.

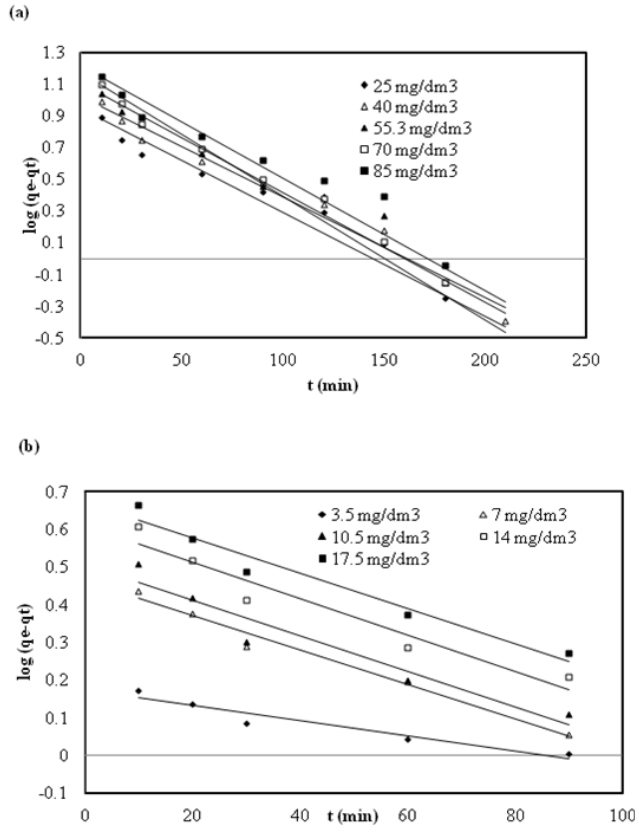

Fig. 6. Lagergren first-order plot for (a) Cr(VI) and (b) Pb removal for different initial feed concentration . pH = 3.5, temperature = 25°C .

Table 5
Kinetic constant parameters obtained for Cr(VI) and Pb by powdered ground nut shell adsorbent

Heavy metal	Pseudo-first-order					Pseudo-second-order				Intraparticle diffusion model		
	C_i (mg/L)	$q_{e,\exp}$ (mg/g)	K_1 (10^{-3}) min^{-1}	$q_{e,cal}$ (mg/g)	R^2	K_2 (10^{-3}) (g/mg min)	$q_{e,cal}$ (mg/g)	h (mg/gh)	R^2	K_{id} (10^{-3}) (mg/g min)	C (mg/g)	R^2
Cr	25	8.5	29.25	3.48	0.957	8.13	7.23	0.42	0.996	0.58	0.422	0.987
	40	12.8	24.9	6.35	0.979	5.61	12.21	83	0.997	0.81	1.63	0.946
	55.3	14.9	36.21	6.8	0.957	6.43	14.31	1.31	0.998	0.76	4.3	0.952
	70	17.3	42.91	7.82	0.963	7.82	16.89	2.23	0.998	0.91	3.99	0.940
	85	19.5	44.02	8.9	0.934	9.21	18.93	3.30	0.997	0.61	9.11	0.940
Pb	3.5	1.23	23.41	7.35	0.926	4.65	0.76	0.0026	0.990	0.10	0.089	0.953
	7	2.31	19.51	10.28	0.980	2.57	1.24	0.00395	0.961	0.19	0.352	0.984
	10.5	2.89	30.28	11.46	0.923	3.62	2.31	0.193	0.990	0.25	0.58	0.971
	14	3.5	37.43	12.56	0.933	3.54	3.14	0.349	0.995	0.29	0.78	0.991
	17.5	4.1	39.22	12.82	0.955	5.86	3.62	0.769	0.991	0.09	5.39	0.984

constant of pseudo-first-order adsorption (min^{-1}). The linearized form of the pseudo-first-order model for the adsorption of Cr(VI) and Pb ions at their various initial concentrations is shown in Figs. 6a and b, respectively. The values of different parameters were calculated and presented in Table 5. The rate constant k_1 was calculated from the slope of plots of $\log(q_e-q_t)$ vs. t and adsorption density q_e was calculated from the intercepts of the plots of $\log(q_e-q_t)$ vs. t. It can be seen from Table 5 that the value of R^2 (0.923–0.98) obtained for the pseudo-first-order kinetic model is not so good, which indicates poor quality of linearization. It indicates the adsorption of Cr(VI) and Pb cannot be well explained by the pseudo-first-order kinetic model. Naushad et al. [38] also not found to fit good the pseudo-first-order equation for removal of Hg^{2+} on $NiFe_2O_4$–NC adsorbent.

3.3.2. Pseudo-second-order equation

As the pseudo-first-order equation could not provide the expected results, the pseudo-second-order adsorption kinetic equation was applied for further analysis. The pseudo-second-order equation is expressed as [39] follows:

$$\frac{dq_t}{dt} = k_2\left(q_e - q_t\right)^2 \tag{3}$$

where q_e and q_t are the sorption capacity at equilibrium and time t, respectively (mg/g), k_2 is the rate constant of the pseudo-second-order adsorption (mg/(g min))

The integrated form of Eq. (3) may be obtained as:

$$\frac{1}{q_e - q_t} = \frac{1}{q_e} + k_2 t \tag{4}$$

which is represent of a pseudo-second-order adsorption. Further, Eq. (4) is written as follows:

$$\frac{t}{q_t} = \frac{1}{k_2 q_e^2} + \frac{t}{q_e} \tag{5}$$

The initial adsorption rate, h (mg/(g min)) is given as

$$h = k_2 q_e^2 \tag{6}$$

Substituting the value of h into Eq. (5), it can be written as

$$\frac{t}{q_t} = \frac{1}{h} + \frac{t}{q_e} \tag{7}$$

The graph between t/q_t vs. t for Eq. (5) is presented in Figs. 7a and b. The value of q_e and k_2 was calculated which are presented in Table 5. The correlation coefficients (R^2) for pseudo-second-order kinetic model has been achieved to near about 0.99. The good values of R^2 indicates that the current adsorption system follows second-order kinetic model. Similar phenomena were also observed by researchers in adsorption process [39–41].

3.3.3. Intraparticle diffusion model

The data obtained during the experiments for the adsorption of Cr(VI) and Pb were also tested for the intraparticle diffusion model to recognize the mechanism participated in the sorption process. Several steps are involved in the adsorption system that are (i) film or surface diffusion, (ii) intraparticle or pore diffusion and (iii) adsorption on the interior sites of the sorbent. The intraparticle diffusion model is expressed as [42,43]:

$$q_t = k_{id} t^{1/2} + C \tag{8}$$

where k_{id} is the intraparticle diffusion rate constant (mg/g $min^{½}$), C is the intercept (mg/g). Figs. 8a and b show the graph of q_t vs. $t^{1/2}$ and the results are given in Table 5. The figure shows three parts. First part is concerned to the diffusion of Cr(VI) and Pb ions from the effluent to the external surface of adsorbent, the second part indicates intraparticle diffusion, and third part shows the ultimate equilibrium stage. The intraparticle diffusion started to slow down the process due to extremely low adsorbate concentrations in

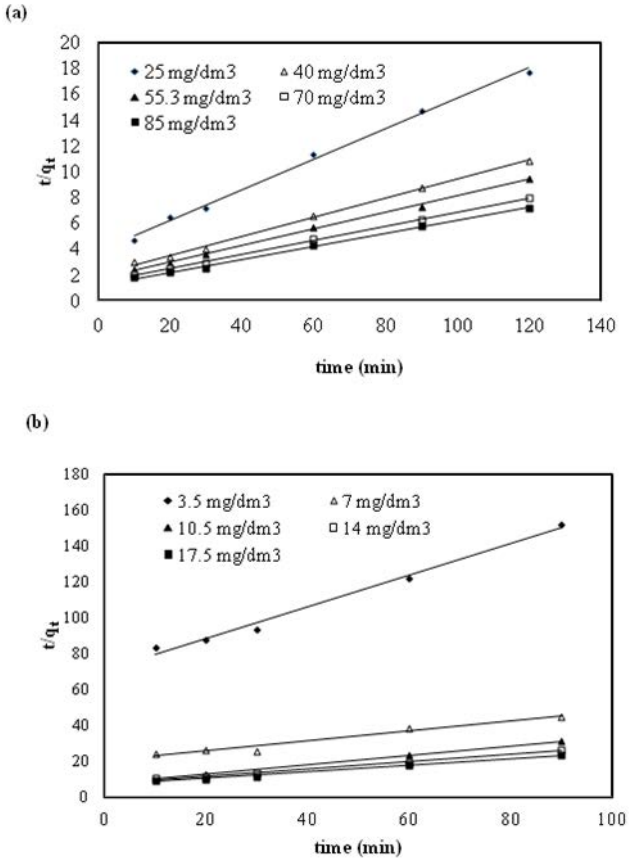

Fig. 7. Pseudo-second-order kinetic plot for (a) Cr(VI) and (b) Pb removal for different initial feed concentration. pH = 3.5, temperature = 25°C.

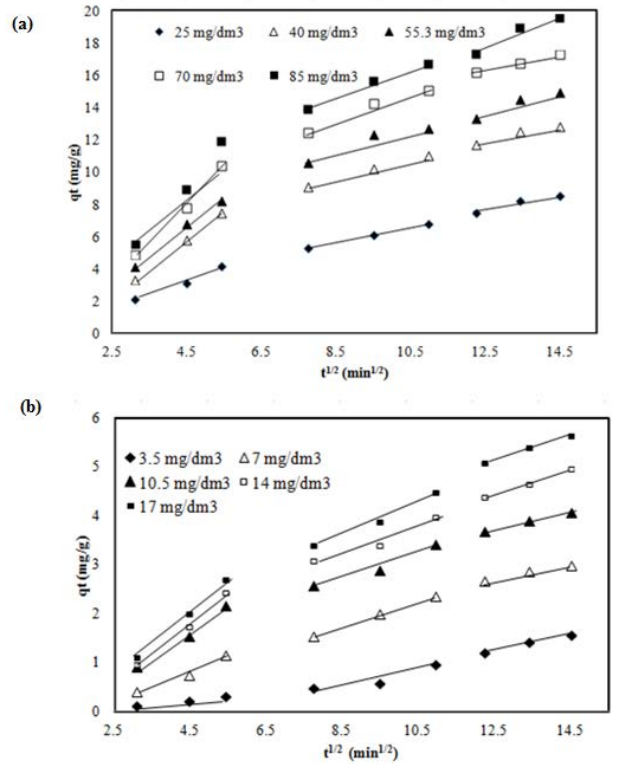

Fig. 8. Intraparticle diffusion kinetic plot for (a) Cr(VI) and (b) Pb removal for different initial feed concentration. pH = 3.5, temperature = 25°C.

the effluent. In general, slope of the line in second stage is called as intraparticle diffusion rate constant (k_{id}) which is presented in Table 5.

3.4. Adsorption isotherm models

To explain the purpose of the fraction of sorbate molecules that are partitioned between liquid and solid phases at equilibrium, adsorption isotherm concepts play very important role. Therefore, different isotherm models were studied for determination of adsorption efficiency. In the present study, three adsorption isotherm models namely (1) Langmuir, (2) Freundlich, and (3) Temkin were undertaken. The Langmuir isotherm model was applied for experimental data to ensure equilibrium condition in the linear form which is expressed as [44]:

$$\frac{C_e}{q_e} = \frac{1}{K_L q_m} + \frac{C_e}{q_m} \tag{9}$$

where C_e is the equilibrium concentration (mg/L) of Cr(VI) and Pb in MPE, q_e is the amount of Cr(VI) and Pb ions adsorbed (mg/g) at equilibrium, q_m represents the maximum theoretical monolayer adsorption capacity (mg/g), and K_L is a constant related to the affinity of adsorption sites (L/mg). The experimental data of Cr(VI) and Pb adsorptions are plotted as C_e/q_e against C_e and presented in Figs. 9a and b. The graphical presentation of C_e/q_e against C_e shows Langmuir adsorption isotherm fitted well to experimental data. Thus, it can be said that the formation of monolayer coverage of the adsorbate on the surface of the adsorbent is suggestable. Langmuir constants q_m and K_L were obtained from the slopes and intercepts of the plots which are presented in Table 6. Data obtained during experiments show high affinity with Langmuir model at different temperature range studied. The adsorption capacity q_m of Cr(VI) was increased from 41.17 to 50.2 mg/g with increasing temperature. Similarly, the adsorption capacity q_m of Pb was increased from 36.07 to 42.811 mg/g with increase in temperature. It reflects that the bonding between metal ions and active sites of the adsorbent increases with temperature. Table 6 also reflects that the K_L values are higher at higher temperatures, showing endothermic nature of both Cr(VI) and Pb adsorption. Similar temperature effects have been reported by different researchers for metal adsorption [45,46].

The Freundlich isotherm is also an important empirical equation to describe the concept of adsorption equilibrium. To get the equilibrium data, initial Cr(VI) and Pb concentrations were varied while the adsorbent mass was kept constant. The equilibrium time of 160 min was used for sorption experiments. The linear form of Freundlich isotherm is expressed as [47]:

$$\ln q_e = \ln K_f + \frac{1}{n} \ln C_e \tag{10}$$

where K_f (mg/g) and 1/n (g/L) are Freundlich adsorption constants, showing the adsorption capacity and adsorption intensity, respectively. The plot between ln q_e against ln C_e shows straight lines Figs. 10a and b. The value of K_f and n was determined from Fig. 10 and results are presented in Table 6. The values R^2 (0.942–0.998) indicate that the Freundlich isotherm fitted well to the experimental data. The Freundlich constant, K_f was increased with temperature, indicating that the adsorption process is endothermic. The high value of n is an indication of the favorability of adsorption [48]. Similar type of result was found by Alqadami et al. [49] for the removal of U(VI)

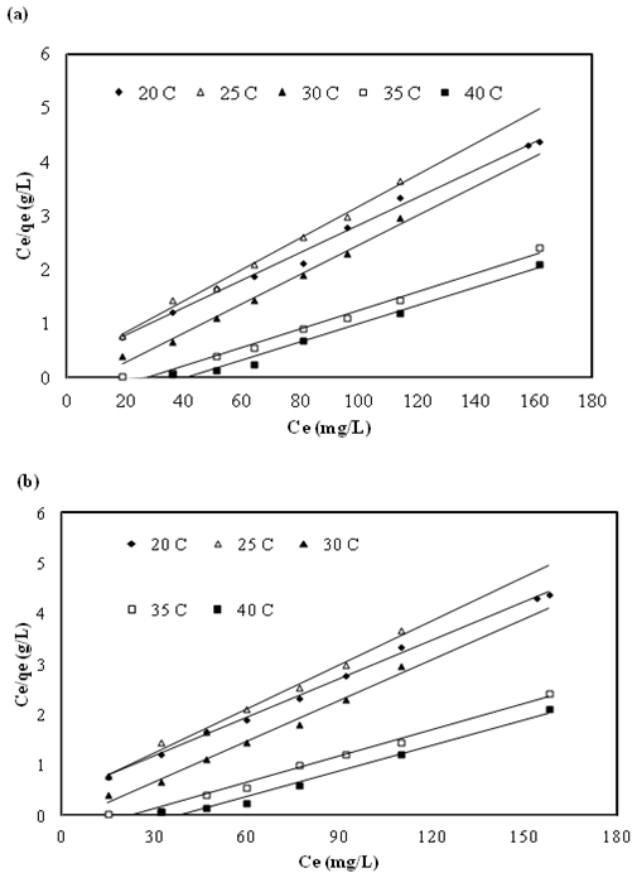

Fig. 9. Langmuir adsorption isotherms for (a) Cr(VI) and (b) Pb removal at different temperatures and pH = 3.5.

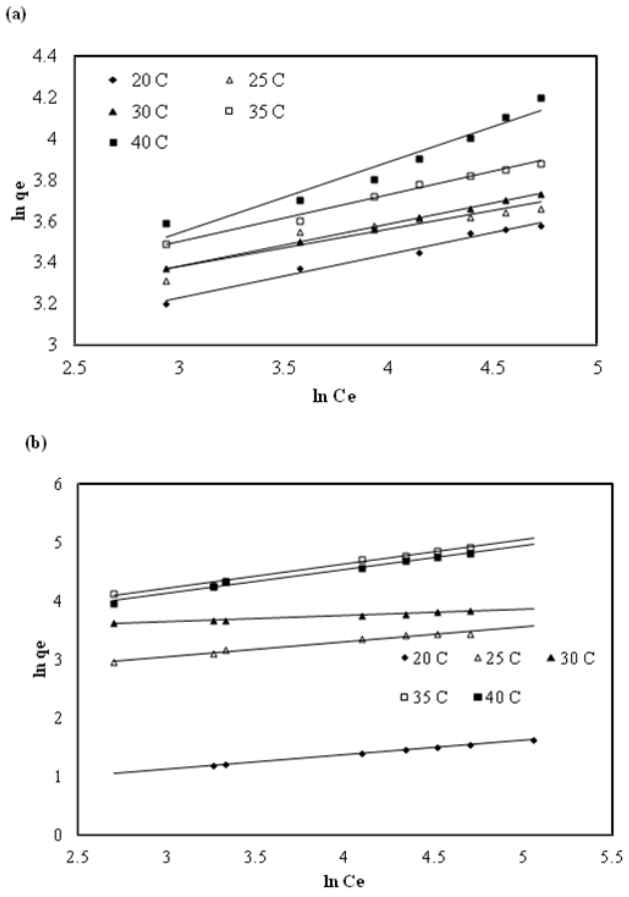

Fig. 10. Freundlich adsorption isotherms for (a) Cr(VI) and (b) Pb removal at different temperatures and pH = 3.5.

Table 6
Langmuir, Freundlich, and Temkin isotherm constants for Cr(VI) and Pb by powdered ground nut shell adsorbent

Heavy metal	T (K)	Langmuir isotherm constants			Freundlich isotherm constants				Temkin isotherm constant
		q_m (mg/g)	K_L (L/mg)	R^2	1/n	N	K_F	R^2	R^2
Cr	298	41.17	0.030	0.993	0.33	2.94	0.19	0.985	0.991
	303	47.5	0.038	0.993	0.32	3.02	0.21	0.971	0.991
	308	48.75	0.044	0.997	0.31	3.15	0.23	0.998	0.983
	313	49.5	0.046	0.987	0.29	3.41	0.245	0.986	0.982
	318	50.2	0.047	0.984	0.34	2.82	0.252	0.942	0.981
Pb	298	36.07	0.024	0.997	0.45	2.1	0.285	0.998	0.985
	303	38.08	0.028	0.992	0.40	2.45	0.412	0.983	0.985
	308	39.48	0.030	0.997	0.31	3.17	0.642	0.983	0.986
	313	41.6	0.031	0.988	0.27	3.62	0.74	0.988	0.984
	318	42.81	0.032	0.983	0.32	3.02	0.82	0.984	0.985

and Th(IV) metal ions on organic frame based composite adsorbent.

The Temkin isotherm model is also a popular method to predict the feasibility of process. This model is based on assumption that the adsorption energy decreases linearly with the surface coverage due to adsorbent–adsorbate interactions. The linear equation of Temkin isotherm model is written as [50]:

$$q_e = \frac{RT}{b_T}\ln K_t + \frac{RT}{b_T}\ln C_e \tag{11}$$

where b_T is the Temkin constant related to the heat of sorption (kJ/mol), K_T is the equilibrium binding constant corresponding to the maximum binding energy (g^{-1}).

The graph between q_e vs. ln C_e for Temkin adsorption isotherm are presented in Figs. 11a and b for Cr(VI) and Pb adsorption, respectively. The Temkin constant b_T was evaluated to 0.50 kJ/mol for Cr(VI) adsorption and 0.45 kJ/mol for Pb adsorption. Similarly K_T was evaluated to 135 L/g for Cr(VI) and 110 L/g for Pb adsorption. Temkin isotherm was found to well fit in term of R^2 value which is presented in Table 6.

3.5. Thermodynamic studies

To determine the feasibility and nature of adsorption process, the different thermodynamic properties such as $\Delta G°$ (standard free energy), $\Delta H°$ (enthalpy change), and $\Delta S°$ (entropy change) were evaluated. The experimental data evaluated based on different temperatures range was used to obtain the thermodynamic parameters. The values of $\Delta H°$ and $\Delta S°$ were calculated from the slopes and intercepts of the plots of ln K_c vs. $1/T$ as shown in Figs. 12a and b using the following equation [51].

$$\ln K_c = \frac{\Delta H°}{RT} + \frac{\Delta S°}{R} \tag{12}$$

The $\Delta G°$ (Gibbs free energy change) was calculated from the following relation.

$$\Delta G° = \Delta H° - T\Delta S° \tag{13}$$

where K_c (m^3/g) is the standard thermodynamic equilibrium constant defined by q_e/C_e. The values of $\Delta G°$, $\Delta H°$, and $\Delta S°$ for Cr(VI) and Pb adsorption are given in Table 7. It can be seen from the table that the value of $\Delta H°$ is positive, indicating that the current adsorption process is endothermic. Furthermore, the value of $\Delta G°$ is negative which shows spontaneity of adsorption process. The decrease in $\Delta G°$ with increase in temperature shows that the adsorption is more favorable at high temperature. Similar type of result has been reported by Alqadami et al. [52] for the adsorption of Cd(II), Cr(III), and Co(II) over nano composite adsorbent.

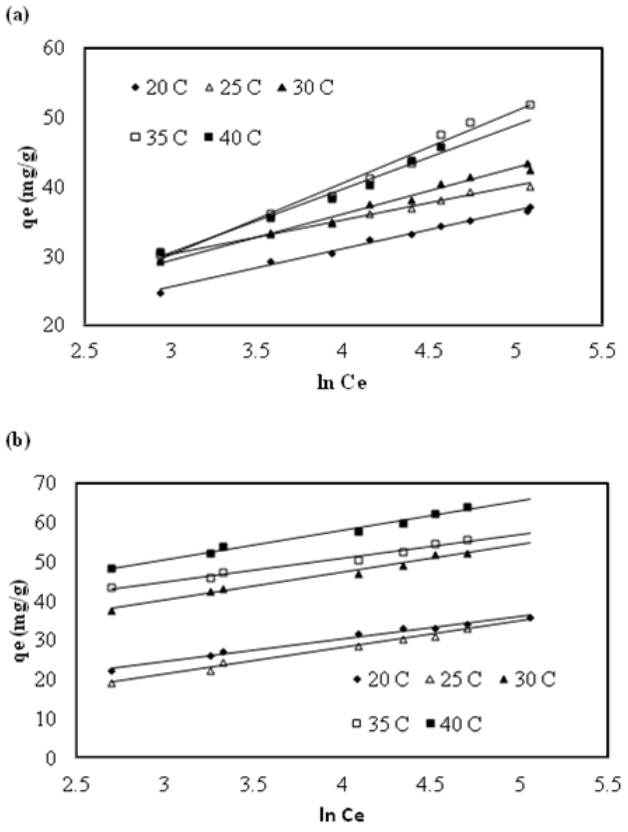

Fig. 11. Temkin adsorption isotherms for (a) Cr(VI) and (b) Pb removal at different temperatures and pH = 3.5.

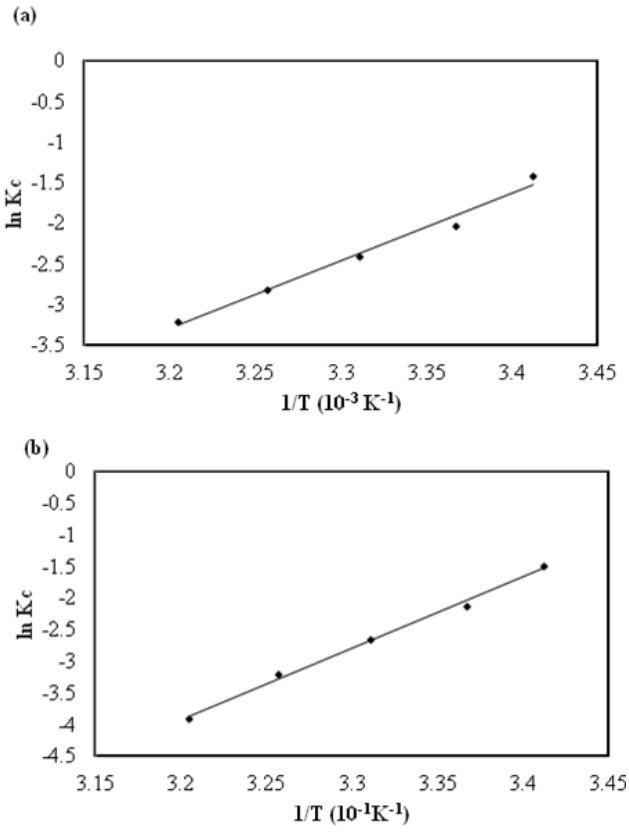

Fig. 12. Plot of ln K_c vs. $1/T$ for (a) Cr(VI) and (b) Pb removal.

Table 7
Thermodynamic parameters for the adsorption of Cr(VI) and Pb on powdered ground nut shell adsorbent at different temperatures

Adsorbent	T (K)	$\Delta G°$ (kJ/mol)	$\Delta H°$ (kJ/mol)	$\Delta S°$ (kJ/mol K)
Powdered ground nut shell	298	–31.21	0.02	0.07
	303	–31.34		
	308	–32.21		
	313	–33.21		

3.6. Adsorption/desorption mechanism

Based on the previous work done by various researchers and based on present studies, the mechanism for the adsorption of Cr(VI) and Pb metals ions onto prepared adsorbent can be explained as the peanut shell has several hydroxyl and carbonyl groups [53]. These groups available as electron-rich species are responsible to donate the electron to the electropositive metal. Therefore, these groups were bonded to the Cr^{2+} and Pb^{2+} metal ion by electrostatic attraction [54]. The charges in Cr^{2+} and Pb^{2+} at different pH changes, and changes in surface properties of adsorbent at different pH has been already explained in section 3.2.1, which was responsible for metal removal at different pH.

4. Conclusion

Adsorbent was prepared from peanut shell by carbonization and chemical activation using $ZnCl_2$, which was found to be very effective for removal of a toxic Cr(VI) and Pb from MPE. The peanut shell is available easily in India hence it can be used as an adsorbent for removal of different metals. In addition, Table 1 demonstrates that prepared adsorbent is better than other adsorbent in term of results, availability and cost. Prepared carbon had good surface area (S_{BET} = 812.43 m^2/g, BJH = 566.12 m^2/g) and contained micropores (1221.55 m^2/g) and mesopores (0.061 cc/g). The removal of Cr (VI) and Pb was observed to be dependent on the initial feed concentration and effluent pH. 94.4% Cr (VI) removal of initial Cr (VI) = 53.3 mg/L and 96.1% Pb removal of initial Pb = 3.5 mg/L were achieved at pH 3.5, temperature 25°C and adsorbent dose 5 g/L. The percentage metal removal was increased with decrease in adsorbent particle size and decreased with decrease in adsorbent dose. The kinetics of Cr(VI) and Pb followed pseudo-second-order rate expression with $R^2 \approx 0.99$. Among three different isotherm model such as Langmuir, Freundlich, and Temkin, the Langmuir adsorption isotherm models fitted well in temperature range studied. Cr(VI) and Pb adsorption on prepared carbon sample was found to be endothermic as q_m and K_L values were higher at higher temperatures. The value of $\Delta G°$ (approximately –33 kJ/mol) was observed negative which shows the feasibility of prepared carbon for the adsorption process.

References

[1] World Health Organization (WHO), Guidelines for Drinking-water Quality, Incorporating First Addendum to 3rd ed., Vol. 1, Recommendations, World Health Organization, Geneva, 2006, p. 595.
[2] M. Zhang, C. Chen, L. Mao, Q. Wu, Use of electroplating sludge in production of fired clay bricks: characterization and environmental risk evaluation, Constr. Build. Mater., 159 (2018) 27–36.
[3] M.A. Martín-Lara, G. Blázquez, M.C. Trujillo, A. Pérez, M. Calero, New treatment of real electroplating wastewater containing heavy metal ions by adsorption onto olive stone, J. Cleaner Prod., 81 (2014) 120–129.
[4] G.S. Simate, N. Maledi, A. Ochieng, S. Ndlovu, J. Zhang, L.F. Walubita, Coal-based adsorbents for water and wastewater treatment, J. Environ. Chem. Eng., 4 (2016) 2291–2312.
[5] S. Kumar, B.C. Meikap, Removal of Chromium(VI) from waste water by using adsorbent prepared from green coconut shell, Desal. Wat. Treat., 52 (2014) 3122–3132.
[6] S.K. Yadav, S. Sinha, D.K. Singh, Chromium(VI) removal from aqueous solution and industrial wastewater by modified date palm trunk, Environ. Prog. Sustainable Energy, 34 (2015) 452–460.
[7] S. Rangabhashiyam, E. Suganya, N. Selvaraju, Packed bed column investigation on hexavalent chromium adsorption using activated carbon prepared from *Swietenia Mahogani* fruit shells, Desal. Wat. Treat., 57 (2015) 13048–13055.
[8] V. Karthik, K. Saravanan, E. Nakkeeran, N. Selvaraju, Biosorption of turquoise blue dye from aqueous solution by dried fungal biomass (*Trichoderma harzianum*) – kinetic, isotherm and thermodynamic studies, Desal. Wat. Treat., 74 (2017) 362–370.
[9] S. Rangabhashiyam, S.N. Selvaraju, Equilibrium and kinetic modeling of chromium (VI) removal from aqueous solution by a novel biosorbent, Res. J. Chem. Environ., 18 (2014) 30–36.
[10] R. Malik, D.S. Ramteke, S.R. Wate, Adsorption of malachite green on groundnut shell waste based powdered activated carbon, Waste Manage., 27 (2007) 1129–1138.
[11] Mu. Naushad, A.A. Ansari, Z.A. ALOthman, J. Mittal, Synthesis and characterization of YVO4:Eu^{3+} nanoparticles: kinetics and isotherm studies for the removal of Cd^{2+} metal ion, Desal. Wat. Treat., 57 (2016) 2081–2088.
[12] A. Mittal, Mu. Naushad, G. Sharma, Z.A. ALOthman, S.M. Wabaidur, M. Alam, Fabrication of MWCNTs/ThO_2 nanocomposite and its adsorption behavior for the removal of Pb(II) metal from aqueous medium, Desal. Wat. Treat., 57 (2016) 21863–21869.
[13] Mu. Naushad, A. ALOthman, Md. R. Awual, M.M. Alam, G.E. Eldesoky, Adsorption kinetics, isotherms, and thermodynamic studies for the adsorption of Pb^{2+} and Hg^{2+} metal ions from aqueous medium using Ti(IV) iodovanadate cation exchanger, Ionics, 21 (2015) 2237–2245.
[14] M. Naushad, Z.A. ALOthman, Inamuddin, H. Javadian, Removal of Pb(II) from aqueous solution using ethylene diamine tetra acetic acid-Zr(IV) iodate composite cation exchanger: kinetics, isotherms and thermodynamic studies, J. Ind. Eng. Chem., 25 (2015) 35–41.
[15] Mu. Naushad, T. Ahamad, Z.A. Alothman, M.A. Shar, N.S. Alhokbany, S.M. Alshehri, Synthesis, characterization and application of curcumin formaldehyde resin for the removal of Cd^{2+} from wastewater: kinetics, isotherms and thermodynamic studies, Ind. Eng. Chem., 29 (2015) 78–86.
[16] Y. Gutha, V.S. Munagapati, Mu. Naushad, K. Abburi, Removal of Ni(II) from aqueous solution by *Lycopersicum esculentum* (Tomato) leaf powder as a low-cost biosorbent, Desal. Wat. Treat., 54 (2015) 200–208.
[17] R. Bushra, Mu. Naushad, R. Adnan, Z.A. Alothman, M. Rafatullah, Polyaniline supported nanocomposite cation exchanger: synthesis, characterization and applications for the efficient removal of Pb^{2+} ion from aqueous medium, J. Ind. Eng. Chem., 21 (2015) 1112–1118.
[18] M. Naushad, Surfactant assisted nano-composite cation exchanger: development, characterization and applications for the removal of toxic Pb^{2+} from aqueous medium, Chem. Eng. J., 235 (2014) 100–108.
[19] M. Ghasemi, Mu. Naushad, N. Ghasemi, Y. Khosravi-fard, A novel agricultural waste based adsorbent for the removal

of Pb(II) from aqueous solution: kinetics, equilibrium and thermodynamic studies, J. Ind. Eng. Chem., 20 (2014) 454–461.
[20] M. Ghasemi, Mu. Naushad, N. Ghasemi, Y. Khosravi-fard, Adsorption of Pb(II) from aqueous solution using new adsorbents prepared from agricultural waste: adsorption isotherm and kinetic studies, J. Ind. Eng. Chem., 20 (2014) 2193–2199.
[21] IS: 1350 (Part 1), Methods of Test for Coal and Coke. Proximate Analysis (Second Revision), Amendment 1,28, Indian Standards Institute, New Delhi, India, 1984.
[22] Z.A. ALOthman, Mu. Naushad, R. Ali, Kinetic, equilibrium isotherm and thermodynamic studies of Cr(VI) adsorption onto low-cost adsorbent developed from peanut shell activated with phosphoric acid, Environ. Sci. Pollut. Res., 20 (2013) 3351–3365.
[23] T.A. Khan, V.V. Singh, Removal of cadmium(II), lead(II), and chromium(VI) ions from aqueous solution using clay, Toxicol. Environ. Chem., 92 (2010) 1435–1446.
[24] M. Ajmal, R.A.K. Rao, R. Ahmad, Adsorption studies of heavy metals on Tectona grandis: removal and recovery of Zn (II) from electroplating wastes, J. Dispersion Sci. Technol., 32 (2011) 851–856.
[25] S. Nag, A. Mondal, U. Mishra, N. Bar, S.K. Das, Removal of chromium(VI) from aqueous solutions using rubber leaf powder: batch and column studies, Desal. Wat. Treat., 57 (2016) 16927–16942.
[26] I.-H. Liao, J.-H. Huang, S.-L. Wang, M.-P. Cheng, J.-C. Liu, Adsorptions of Cd(II) and Pb(II) in aqueous solution by rice-straw char, Desal. Wat. Treat., 57 (2016) 21619–21626.
[27] Z.A. ALOthman, R. Ali, Mu. Naushad, Hexavalent chromium removal from aqueous medium by activated carbon prepared from peanut shell: adsorption kinetics, equilibrium and thermodynamic studies, Chem. Eng. J., 184 (2012) 238–247.
[28] D. Vasanth, G. Pugazhenthi, R. Uppaluri, Biomass assisted microfiltration of chromium(VI) using Baker's yeast by ceramic membrane prepared from low cost raw materials, Desalination, 285 (2012) 239–244.
[29] https://chem.libretexts.org/Bookshelves/General_Chemistry.
[30] U. Maheshwari, S. Gupta, Removal of Cr(VI) from wastewater using activated neem bark in a fixed-bed column: interference of other ions and kinetic modelling studies, Desal. Wat. Treat., 57 (2016) 8514–8525.
[31] B. Saha, C. Orvig, Biosorbents for hexavalent chromium elimination from industrial and municipal effluents, Coord. Chem. Rev., 254 (2010) 2959–2972.
[32] S. Suganya, K. Kayalvizhi, P. Senthil Kumar, A. Saravanan, V.V. Kumar, Biosorption of Pb(II), Ni(II) and Cr(VI) ions from aqueous solution using *Rhizoclonium tortuosum*: extended application to nickel plating industrial wastewater, Desal. Wat. Treat., 57 (2016) 25114–25139.
[33] K.J. Cronje, K. Chetty, M. Carsky, J.N. Sahu, B.C. Meikap, Optimization of chromium(VI) sorption potential using developed activated carbon from sugarcane bagasse with chemical activation by zinc chloride, Desalination, 275 (2011) 276–284.
[34] K.M. Sreenivas, M.B. Inarkar, S.V. Gokhale, S.S. Lele, Re-utilization of ash gourd (*Benincasa hispida*) peel waste for chromium (VI) biosorption: equilibrium and column studies, J. Environ. Chem. Eng., 2 (2014) 455–462.
[35] S. Wang, H. Li, Kinetic modeling and mechanism of dye adsorption on unburned carbon, Dyes Pigm., 72 (2007) 308–314.
[36] S. Rangabhashiyam, M.S. Giri Nandagopal, E. Nakkeeran, N. Selvaraju, Adsorption of hexavalent chromium from synthetic and electroplating effluent on chemically modified *Swietenia mahagoni* shell in a packed bed column, Environ. Monit. Assess., 188 (2016) 2–13.
[37] M.H. Fatehi, J. Shayegan, M. Zabihi, I. Goodarznia, Functionalized magnetic nanoparticles supported on activated carbon for adsorption of Pb(II) and Cr(VI) ions from saline solutions, J. Environ. Chem. Eng., 5 (2017) 1754–1762.
[38] Mu. Naushad, T. Ahamad, B.M. Al-Maswari, A.A. Alqadami, S.M. Alshehri, Nickel ferrite bearing nitrogen-doped mesoporous carbon as efficient adsorbent for the removal of highly toxic metal ion from aqueous medium, Chem. Eng. J., 330 (2017) 1351–1360.
[39] J. Yu, C. Jiang, Q. Guan, P. Ning, J. Gu, Q. Chen, J. Zhang, R. Miao, Enhanced removal of Cr(VI) from aqueous solution by supported ZnO nanoparticles on biochar derived from waste water hyacinth, Chemosphere, 195 (2018) 632–640.
[40] Y.S. Ho, G. Mckay, D.A.J. Wase, C.F. Forster, Study of the sorption of divalent metal ions on to peat, Adsorpt. Sci. Technol., 18 (2000) 639–650.
[41] I. Enniya, L. Rghioui, A. Jourani, Adsorption of hexavalent chromium in aqueous solution on activated carbon prepared from apple peels, Sustainable Chem. Pharm., 7 (2018) 9–16.
[42] D. Sarkar, S.K. Das, P. Mukherjee, A. Bandyopadhyay, Proposed adsorption–diffusion model for characterizing chromium(VI) removal using dried water hyacinth roots, Clean Soil Air Water, 38 (2010) 764–770.
[43] T. Shi, D. Yang, H. Yang, J. Ye, Q. Cheng, Preparation of chitosan crosslinked modified silicon material and its adsorption capability for chromium(VI), Appl. Clay Sci., 142 (2017) 100–108.
[44] P.K. Sharma, S. Ayub, C.N. Tripathi, Isotherms describing physical adsorption of Cr(VI) from aqueous solution using various agricultural wastes as adsorbents, Cogent Eng., 3 (2016) 1–20.
[45] P.S. Kumar, S. Ramalingam, R.V. Abhinaya, S.D. Kirupha, A. Murugesan, S. Sivanesan, Adsorption of metal ions onto the chemically modified agricultural waste, Chem. Eng. J., 167 (2011) 122–131.
[46] P.S. Kumar, S. Ramalingam, V. Sathyaselvabala, S.D. Kirupha, S. Sivanesan, Removal of copper(II) ions from aqueous solution by adsorption using cashew nut shell, Desalination, 266 (2011) 63–71.
[47] N. Daneshvar, D. Salari, S. Aber, Chromium adsorption and Cr(VI) reduction to trivalent chromium in aqueous solutions by soya cake, J. Hazard. Mater., 94 (2002) 49–61.
[48] V.C. Srivastava, I.D. Mall, I.M. Mishra, Removal of cadmium(II) and zinc(II) metal ions from binary aqueous solution by rice husk ash, Colloids Surf., A, 312 (2008) 172–184.
[49] A.A. Alqadami, Mu. Naushad, Z.A. Alothman, A.A. Ghfar, Novel metal–organic framework (MOF) based composite material for the sequestration of U(VI) and Th(IV) metal ions from aqueous environment, ACS Appl. Mater. Interfaces, 9 (2017) 36026–36037.
[50] D.H. Lataye, I.M. Mishra, I.D. Mall, Adsorption of α-picoline onto rice husk ash and granular activated carbon from aqueous solution: equilibrium and thermodynamic study, Chem. Eng. J., 147 (2009) 139–149.
[51] S. Suresh, V.C. Srivastava, I.M. Mishra, Isotherm, thermodynamics, desorption, and disposal study for the adsorption of catechol and resorcinol onto granular activated carbon, J. Chem. Eng. Data, 56 (2011) 811–818.
[52] A.A. Alqadami, Mu. Naushad, M.A. Abdalla, T. Ahamad, Z.A. ALOthman, S.M. Alshehri, A.A. Ghfar, Efficient removal of toxic metal ions from wastewater using a recyclable nanocomposite: a study of adsorption parameters and interaction mechanism, J. Cleaner Prod., 156 (2017) 426–436.
[53] M.E. Ossman, M.S. Mansour, M.A. Fattah, N. Taha, Y. Kiros, Peanut shells and talc powder for removal of hexavalent chromium from aqueous solutions, Bulg. Chem. Commun., 46 (2014) 629–639.
[54] Mu. Naushad, T. Ahamad, G. Sharma, A.H. Al-Muhtaseb, A.B. Albadarin, M.M. Alam, Z.A. ALOthman, S.M. Alshehri, A.A. Ghfar, Synthesis and characterization of a new starch/SnO_2 nanocomposite for efficient adsorption of toxic Hg^{2+} metal ion, Chem. Eng. J., 300 (2016) 306–316.